

Tuning the Temperature Domain of Phonon Drag in Thin Films by the Choice of Substrate

Guoyu Wang,¹ Lynn Endicott,¹ Hang Chi,¹ Peter Loš'ák,² and Ctirad Uher^{1,*}

¹*Department of Physics, University of Michigan, Ann Arbor, Michigan 48109, USA*

²*Faculty of Chemical Technology, University of Pardubice, Čs. Legií Square 565, 53210 Pardubice, Czech Republic*

(Received 2 November 2012; published 26 July 2013)

At low temperatures, in reasonably pure conductors subjected to a thermal gradient, charge carriers (electrons and holes) are swept (dragged) by out of equilibrium phonons, giving rise to a large contribution to the Seebeck coefficient called phonon drag. We demonstrate a spectacular influence of substrate phonons on charge carriers in thin films of Bi₂Te₃. We show that one can control and tune the position and magnitude of the phonon-drag peak over a wide range of temperatures by depositing thin films on substrates with vastly different Debye temperatures. Our experiments also provide a way to study the nature of the phonon spectrum in thin films, which is rarely probed but clearly important for a complete understanding of thin film properties and the interplay of the substrate and films.

DOI: [10.1103/PhysRevLett.111.046803](https://doi.org/10.1103/PhysRevLett.111.046803)

PACS numbers: 73.50.Lw, 63.22.Np, 73.61.Le

Phonons “leaking” [1] from a substrate to a thin film have long been recognized as a mechanism contributing to large anomalies in measurements of the Seebeck coefficient (often called the thermopower) at low temperatures. Spurred by the discovery of the quantum Hall effect, numerous studies of the Seebeck coefficient in GaAs/Al_xGa_{1-x}As heterostructures [2,3] and Si-metal-oxide-semiconductor field-effect transistors (MOSFET’s) [4–6], have been carried out since the mid-1980s and they often resulted in exceptionally large Seebeck coefficients with values exceeding millivolt/K at liquid helium temperatures. Such large magnitudes of the Seebeck coefficient are a manifestation of the electron-phonon interaction otherwise known as the phonon-drag effect [7,8]. In this process, nonequilibrium phonons generated in the substrate material as a result of an imposed thermal gradient are leaking into the 2D layer of the heterostructure and interact with the 2D electron system. Phonons impart their momentum to electrons resulting in an electric current just as an applied electric field would do. However, under the condition of net zero electric current (experimental condition under which the Seebeck coefficient is measured), an electric field is set up that counters the impulsively generated flow of electrons. By the phonon-drag Seebeck coefficient one understands the ratio of this induced electric field to the imposed thermal gradient. Unlike the diffusion Seebeck coefficient that is present at all temperatures, the phonon-drag contribution is manifested only at temperatures where electron-phonon processes dominate over all other modes of phonon scattering. In practice, this implies low enough temperatures where phonon-phonon Umklapp processes are infrequent, but temperatures not so low that the population of phonons would be very small. Expressions for the phonon-drag thermopower of both bulk [9] and lower-dimensional semiconducting structures, including the temperature dependence of the effect [10,11], have been worked out and applied to experimental

data. Specifically, for 2D heterostructures, the induced phonon-drag electric field can be written in a physically intuitive form: [12]

$$\mathbf{E}_{\text{ph}} = \sum_s \frac{m^* \nu_s \Lambda_s}{eT\tau_{\text{ep}}^s} \nabla T, \quad (1)$$

where m^* is the effective mass, ν_s is the velocity of the acoustic phonon mode s , Λ_s is the phonon mean-free path, τ_{ep}^s is the electron-phonon relaxation time for scattering by the mode s , and the summation is taken over the appropriate acoustic modes.

In all studies of the low temperature Seebeck effect in lower-dimensional structures [2–6], and even in the recently discovered spin Seebeck effect in Mn-doped GaAs films [13,14], the active 2D layer had similar composition and structure to the substrate. While this is a desirable feature from the perspective of growing high quality epitaxial layers, the fact that the substrate and the film have essentially the same phonon characteristics curtails a spectrum of information one can gain regarding interactions of substrate phonons with charge carriers of the film. Specifically, issues such as the influence of the Debye temperature and the possibility of tuning the position of the phonon-drag peak are inaccessible in such studies.

In this research we focus on the influence substrate phonons exert on the Seebeck coefficient of films where the substrate and the film are different materials. As a film structure, we chose epitaxial films of Bi₂Te₃. Beyond the fact that Bi₂Te₃ is the best room temperature thermoelectric [15] and the favored material for studies of topological insulators [16,17], its distinctly layered structure typified by quintuple layer (QL) of $-\text{Te}^{(2)}-\text{Bi}-\text{Te}^{(1)}-\text{Bi}-\text{Te}^{(2)}-$ and weak, van der Waals bonds between the neighboring stacks [see Fig. 1(a)] makes Bi₂Te₃ an excellent candidate for the van der Waals-type epitaxy [18]. This ensures that c -axis oriented thin films can be grown on many different substrates [19–21]. Specifically, we chose BaF₂ (111) and

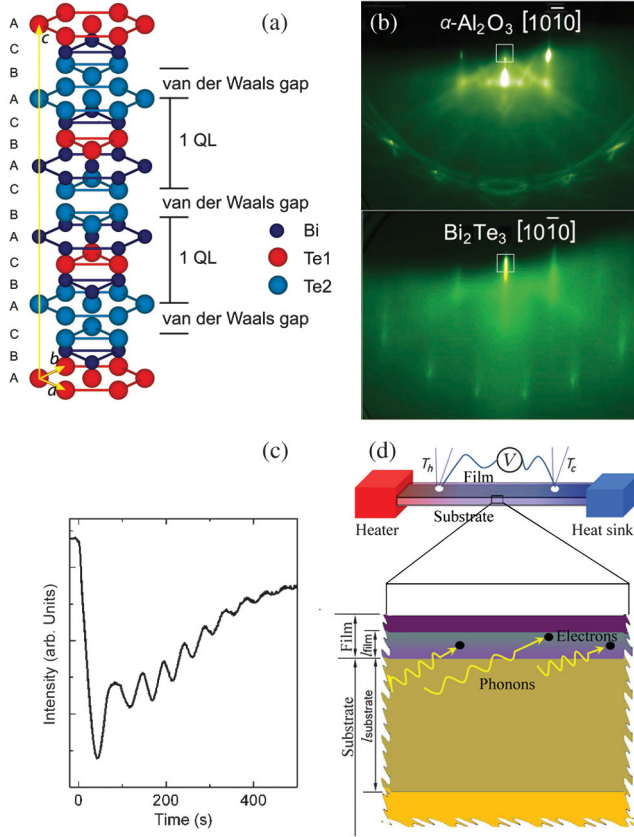


FIG. 1 (color). (a) Hexagonal model of the structure for Bi_2Te_3 . (b) RHEED pattern for sapphire substrate and Bi_2Te_3 film. (c) Profile of (0,0) area RHEED intensity. The area is indicated with the white box in (b). (d) Schematic picture for the phonon-drag process in a film (not to scale).

sapphire (0001), substrates with vastly different Debye temperatures of 287 and 980 K, respectively. Films with thickness spanning from 6 to 1000 nm were deposited using molecular beam epitaxy with growth parameters and structural properties described previously [22]. For comparison, we have also included a single crystal Bi_2Te_3 in the study

[23]. Details concerning transport measurements are also given in Ref. [22]. Briefly, the transport parameters were measured using a steady state technique over 2–300 K on rectangular-shaped samples of $10 \times 1 \times 0.5 \text{ mm}^3$. One end of the sample was clamped to a copper heat sink while the other end was provided with a miniature chip resistor serving as the heater. The temperature difference was measured with two Cernox thermometers embedded in small copper tubes with a fine lip glued with Stycast to the backside of the substrate. Voltages were measured with Keithley 2182A nanovoltmeters using two fine copper wires carefully soldered to the film directly opposite the contacts of the thermometers. Temperature difference was kept below 5% of the absolute measurement temperature. The Seebeck coefficient was corrected for the thermopower of copper. Accuracy of all the transport measurements was better than 5%.

The epitaxial nature and quality of the films is illustrated in Fig. 1. The sharp stripes in the reflection high-energy electron diffraction (RHEED) pattern depicted in Fig. 1(b) indicate a smooth film surface and oscillations in the RHEED signal in Fig. 1(c) confirm a 2D growth mode. The XRD data (not shown here) corroborate the c -axis orientation of films. A summary of transport data is given in Table I.

The temperature dependence of the absolute value of Seebeck coefficients for 9 nm films deposited on BaF_2 and sapphire as well as the Seebeck coefficient of a bulk single crystal Bi_2Te_3 are shown in Fig. 2(a). A small but clearly distinguished phonon-drag contribution observed on a single crystal at 7 K is to be contrasted with an order of magnitude larger phonon-drag in the two film structures with peak positions at 14 (BaF_2 substrate) and 31 K (sapphire substrate). We stress that, apart from the same thickness, the two films have also similar carrier densities and mobilities. Consequently, the very different positions of the phonon-drag peak observed in films on BaF_2 and on sapphire have nothing to do with the films' electronic properties. One may also consider strain as the driving force for

TABLE I. Transport parameters of Bi_2Te_3 thin films with different thickness on sapphire and BaF_2 substrates. T_p indicates the position of the phonon-drag peak.

	Film thickness (nm)	$n(5 \text{ K})$ (10^{19} cm^{-3})	$\rho(5 \text{ K})$ ($\mu \Omega \text{ m}$)	$\mu(5 \text{ K})$ ($10^3 \text{ cm}^2/\text{V s}$)	T_p (K)	$S(300 \text{ K})$ ($\mu \text{ V}/\text{K}$)
Films on sapphire	6	-11.8	3.3	0.16	29	-71
	9	-6.8	1.5	0.62	31	-103
	15	-5.5	1.9	0.6	28	-125
	24	-3.2	1.7	1.1	29	-142
	45	-1.4	1.6	2.9	30	-171
	190	-0.91	1.1	6.1	26	-235
	1000	-0.45	2.1	6.7	31	-257
Films on BaF_2	9	-8.8	3.0	0.23	14	-147
	24	-2.1	1.15	2.6	14	-221
Bulk single crystal	Bulk	1.58	0.47	8.4	7	245

the shift of the phonon drag peak temperature. However, as shown in Fig. S1(c), the strain in Bi_2Te_3 films grown on Al_2O_3 substrates is released very fast due to the weak interaction between QLs, and the in-plane lattice parameter attains its normal value of Bi_2Te_3 after the growth of only 2 QLs. Therefore, a rebound of the phonon-drag peak position to 7 K would be expected when the film thickness is greater than 10 nm. This does not happen even in films with the thickness of 190 nm. Moreover, the lattice mismatch between BaF_2 and Bi_2Te_3 is only 0.1% and the difference in the thermal expansion coefficients leads to no more than about 0.1% lattice difference over the range of 300 K [24]; yet a sizable shift in the phonon-drag peak temperature is observed. The above two points effectively rule out a possibility that strain plays a major role in the shifted phonon-drag peak position. Rather, as Fig. 2(b) clearly reveals, the position of the phonon-drag peaks closely follows the position of the peak in the thermal conductivity of the respective substrates. This also holds for the bulk Bi_2Te_3 single crystal sample. Such agreement between the position of peaks in the Seebeck coefficient and the thermal conductivity indicates a significant contribution of “leaking” substrate acoustic phonons interacting with charge carriers of the films. The process is most effective at temperatures where there is the largest concentration of heat-carrying phonons that can interact with carriers which is near the peak in the thermal conductivity. At temperatures above the peak in the thermal conductivity, Umklapp processes dissipate phonon momenta. At temperatures much below the peak, the density of available phonons decreases and their favored scattering targets are sample boundaries rather than charge carriers. This general trend is controlled by the Debye temperature of the substrate that specifies temperature regimes where the respective phonon scattering processes dominate. Clearly, the presence of a substrate, through its phonon spectrum, influences the electron-phonon interaction in a deposited semiconducting film which, in turn, governs the strength and the temperature domain of the phonon-drag effect. While searching for references to prior work, we came across a Letter of Underwood *et al.* [25] who found an almost negligible effect of a substrate on the electron-phonon coupling in metallic films well below 1 K. This contrasting finding with our results is perhaps not surprising because of vastly different temperature regimes. At sub-Kelvin temperatures the charge carriers are in no way the dominant scatterer of phonons and thus the electron-phonon coupling ought to be very weak.

Substrate acoustic phonons that can interact with charge carriers and drag them along are those with phonon wave vectors restricted to $q \leq 2k_F$, where k_F is the Fermi wave vector of charge carriers. Moreover, such phonons should be excited within a penetration depth of the film-substrate interface. The mean-free paths for sapphire, BaF_2 , as well as for Bi_2Te_3 [24] are plotted in Fig. 2(c). Even if sample size may limit the mean-free path of phonons at low temperatures,

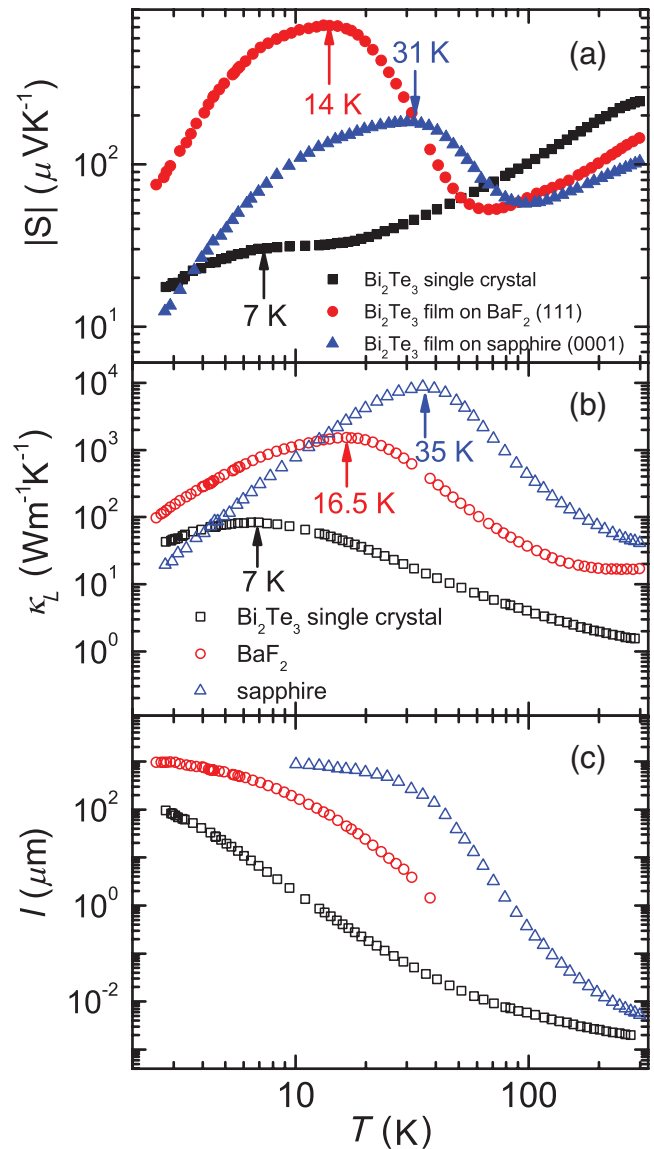


FIG. 2 (color). (a) Temperature dependence of the Seebeck coefficient for Bi_2Te_3 single crystal, 9 nm Bi_2Te_3 films on BaF_2 (red), and sapphire (blue) substrates. (b) The thermal conductivity of a bare sapphire substrate and a bare BaF_2 substrate. Being both insulators, the data represent the lattice contribution. For the Bi_2Te_3 single crystal, we show the lattice thermal conductivity by subtracting the electron contribution from the total thermal conductivity via the Wiedemann-Franz law. (c) Phonon mean free path for Bi_2Te_3 single crystal, BaF_2 , and sapphire.

there is a huge difference between the free paths in Bi_2Te_3 and the two respective substrates. For instance, near 31 K where the phonon-drag peaks in the film on sapphire, the mean-free path of phonons in the substrate is some five thousand times longer than in the film itself. Even though the film-substrate interface may scatter some phonons, the very large mean-free path of phonons in the substrate means that there is a vast reservoir of acoustic phonons capable of interacting with charge carriers in the film and those that leak into the film will do so effectively. A schematic of this

process is shown in Fig. 1(d). Since the leaking phonons reflect the lattice dynamics of a substrate rather than that of a film, they will impose their birthmark on charge carriers in the film, alter the domain of electron-phonon interaction, and shift the peak position of the phonon-drag Seebeck coefficient towards a temperature where the thermal conductivity of the substrate peaks. This is clearly demonstrated by the phonon-drag data of Bi_2Te_3 films on both substrates. In the case of a bulk single crystal Bi_2Te_3 , there is no substrate. It is acoustic phonons in Bi_2Te_3 that dominate the heat transport, dragging the carriers; thus, the thermal conductivity and phonon-drag peaks coincide.

Since it is substrate phonons which dominate the phonon-drag process in thin Bi_2Te_3 films, any factor that affects substrate phonons should also influence the film's phonon-drag peak. To check this point, we grew 9 nm Bi_2Te_3 films simultaneously on two sapphire substrates with thicknesses of 0.5 and 0.1 mm, i.e., subject to the exact same growth conditions and component fluxes. Figure 3 shows the Seebeck coefficient of the films as well as the thermal conductivity of the two bare substrates with differing thickness as a function of temperature. Note that the thermal conductivity curves overlap at higher temperatures; however, at low temperatures, the boundary scattering of phonons in the thinner substrate is stronger relative to the thicker substrate, and this attenuates the low-temperature portion of the thermal conductivity curve in the former. Since boundary scattering of phonons is strong at low temperatures but weak at high temperatures, logically this leads to an effective increase of the peak temperature in thermal conductivity, in our case from 35 to 39 K. The high temperature Seebeck coefficients (shown) and the electrical resistance (not shown) also overlap. Additionally, at low temperatures, the stronger phonon boundary scattering in the thinner substrate decreases the momentum that can be transferred from phonons to electrons, and leads to a lower phonon-drag Seebeck effect. For

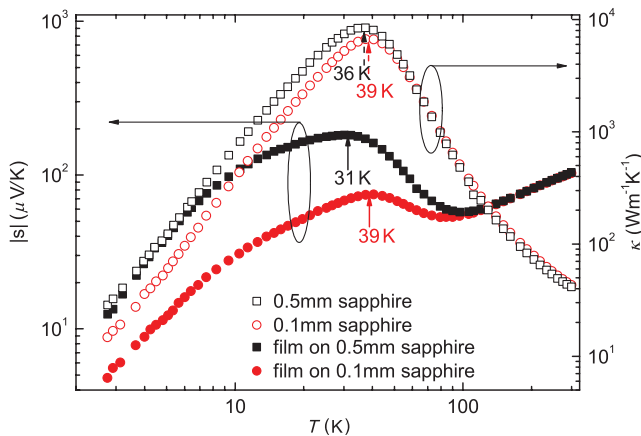


FIG. 3 (color). Temperature dependence of the Seebeck coefficients (left axis) for two 9 nm films grown on sapphire substrates with thickness of 0.5 and 0.1 mm, respectively. The thermal conductivities (right axis) of two substrates are also shown.

the same reasons mentioned above, the peak temperature of the phonon-drag coefficient also increases with decreasing substrate thickness, in our case from 31 to 39 K.

In general, one would expect the leaking phonons to be particularly effective in very thin films with the thickness significantly less than the penetration depth of such phonons. As film thickness increases, a smaller fraction of the film volume would be accessible to the leaking phonons before they are scattered and the strength of the phonon-drag should weaken. To test this premise, we deposited Bi_2Te_3 films with the thickness in the range of 6–1000 nm on sapphire and measured their transport properties. Although the film on the BaF_2 substrate in Fig. 2(a) shows a higher phonon-drag peak, and therefore might be a better substrate on which to study this phenomena, the brittleness of BaF_2 and the fragility to thermal shock make it an inconvenient choice. To minimize the effect of different carrier densities of different films, we normalize the Seebeck coefficient to its value at 200 K, as shown in Fig. 4(a). The most striking feature of the data is a strong dependence of the magnitude of the phonon-drag peak on the film thickness while the temperature where the peak occurs is thickness independent. The thinnest Bi_2Te_3 sample (6 nm) possesses the peak value an order of magnitude larger than samples with the thickness of 45 and 190 nm. Based on the Mott's formula for degenerate semiconductors, the phonon-drag term can be calculated by subtracting the diffuse term (linear temperature dependence) from the total Seebeck value. To do so, we assume that the phonon-drag contribution vanishes at 200 K, which

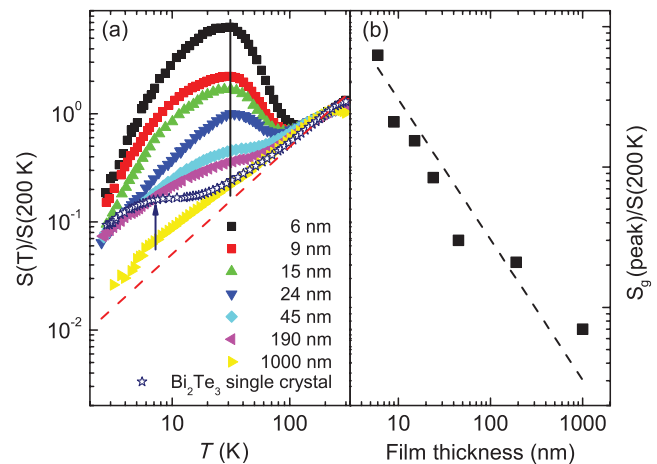


FIG. 4 (color). (a) Temperature dependence of the Seebeck coefficient (normalized to the value at 200 K) for Bi_2Te_3 films with different thickness on sapphire (0001) substrate. Data for Bi_2Te_3 single crystal are also presented for comparison. The red dashed line indicates the linear temperature dependence of diffuse Seebeck coefficient. The solid vertical line indicates the phonon-drag peak position for films. Arrow indicates the phonon-drag peak in bulk Bi_2Te_3 . (b) The peak value of the phonon-drag Seebeck coefficient (normalized to the Seebeck value at 200 K) for films with different thickness on the sapphire substrate.

is not an unreasonable approximation for the range of carrier densities of 10^{19} – 10^{20} cm^{-3} .

Peak values of the phonon-drag Seebeck coefficient (normalized to the Seebeck value at 200 K) as a function of thickness are shown in Fig. 4(b). The phonon-drag contribution decreases monotonically with increasing thickness, indicating decreasing influence of substrate phonons in the thicker films. Assuming that the decay of substrate phonons with the increasing film thickness shares similar functional form with the light intensity distribution in a medium, the phonon flux intensity at thickness t can be written as $F(t) = F_0 e^{-\alpha t}$, where F_0 is the flux intensity at $t = 0$ (at the interface), and α is the decay constant (similar to the absorption coefficient when light passes through a medium). For a film with thickness t_0 , the measured Seebeck signal $S_g(t_0)$ should be the weighted average of the Seebeck coefficient at different thicknesses, with local electrical conductance $\sigma(t)$ as the weight: $S_g(t_0) = (\int_0^{t_0} \sigma(t) s_g(t) dt) / (\int_0^{t_0} \sigma(t) dt)$, where $s_g(t)$ is the phonon-drag Seebeck coefficient at the depth t from the interface, which should be proportional to the phonon flux density at this thickness, $F(t)$. Assuming the simplest situation where $\sigma(t)$ is constant (in fact the normalization already takes care of the carrier density and mobility difference between films with different thickness), one will get

$$S_g(t_0) \propto (1 - e^{-\alpha t_0}) / \alpha t_0. \quad (2)$$

Fitting the thickness dependence of the phonon-drag Seebeck coefficient to this equation, we obtain the dashed line in Fig. 4(b) and the fitting parameter $\alpha \sim 10 \text{ nm}^{-1}$ (corresponding to the penetration depth of 0.1 nm). This means that the phonon flux “leaking” from the substrate decays rather quickly in the film, explaining the rapid decrease in the phonon-drag magnitude with the increasing film thickness.

In conclusion, we find that phonons leaking from the substrate strongly affect the carrier dynamics of the film and cause a large phonon-drag peak on the Seebeck curve. The position of this peak correlates with the maximum on the thermal conductivity of the substrate and is governed by the nature of the substrate, namely, by the Debye temperature Θ_D . The peak height of this substrate-related phonon drag can be very large for very thin films, but decreases very fast with increasing film thickness. Our research demonstrates that one can manipulate the temperature where the phonon-drag effect dominates by selecting a suitable substrate material. This result provides a way to probe the electron-phonon coupling in thin film structures and demonstrates the influence of substrates on phonon and electronic properties of thin films.

This research work was supported by the Center for Solar and Thermal Energy Conversion, an Energy Frontier Research Center funded by the U.S. Department of Energy, Office of Science, Office of Basic Energy Sciences under Grant No. DE-SC0000957.

*To whom correspondence should be addressed.

cuh@umich.edu

- [1] M. A. Zudov, I. V. Ponomarev, A. L. Efros, R. R. Du, J. A. Simmons, and J. L. Reno, *Phys. Rev. Lett.* **86**, 3614 (2001).
- [2] R. Fletcher, M. D’Iorio, A. S. Sachrajda, R. Stoner, C. T. Foxon, and J. J. Harris, *Phys. Rev. B* **37**, 3137 (1988).
- [3] R. Fletcher, J. J. Harris, C. T. Foxon, M. Tsaousidou, and P. N. Butcher, *Phys. Rev. B* **50**, 14991 (1994).
- [4] R. Fletcher, V. M. Pudalov, Y. Feng, M. Tsaousidou, and P. N. Butcher, *Phys. Rev. B* **56**, 12422 (1997).
- [5] S. Agan, O. A. Mironov, E. H. C. Parker, and T. E. Whall, *Semicond. Sci. Technol.* **15**, 551 (2000).
- [6] N. V. Zavaritsky, *Physica (Amsterdam)* **126B&C**, 369 (1984).
- [7] R. Fletcher, E. Zaremba, and U. Zeitler, in *Electron-Phonon Interactions in Low-Dimensional Structures*, edited by L. Challis (Oxford University Press, Oxford, 2003), Chap. 5.
- [8] B. L. Gallagher and P. N. Butcher, in *Handbook on Semiconductors*, edited by P. T. Landsberg (Elsevier, Amsterdam, 1992), Vol. 1, p. 817.
- [9] C. Herring, *Phys. Rev.* **96**, 1163 (1954).
- [10] H. L. Stormer, L. N. Pfeiffer, K. W. Baldwin, and K. W. West, *Phys. Rev. B* **41**, 1278 (1990).
- [11] S. K. Lyo, *Phys. Rev. B* **38**, 634 (1988).
- [12] A. Miele, R. Fletcher, E. Zaremba, Y. Feng, C. T. Foxon, and J. J. Harris, *Phys. Rev. B* **58**, 13181 (1998).
- [13] C. M. Jaworski, J. Yang, S. Mack, D. D. Awschalom, J. P. Heremans, and R. C. Myers, *Nat. Mater.* **9**, 898 (2010).
- [14] C. M. Jaworski, J. Yang, S. Mack, D. D. Awschalom, R. C. Myers, and J. P. Heremans, *Phys. Rev. Lett.* **106**, 186601 (2011).
- [15] H. J. Goldsmid, *Electronic Refrigeration* (Pion, London, 1986).
- [16] Y. L. Chen, J. G. Analytis, J.-H. Chu, Z. K. Liu, S.-K. Mo, X. L. Qi, H. J. Zhang, D. H. Lu, X. Dai, Z. Fang, S. C. Zhang, I. R. Fisher, Z. Hussain, Z.-X. Shen, *Science* **325**, 178 (2009).
- [17] H. Zhang, C.-X. Liu, X.-L. Qi, X. Dai, Z. Fang, and S.-C. Zhang, *Nat. Phys.* **5**, 438 (2009).
- [18] A. Koma, K. Sunouchi, and T. Miyajima, *J. Vac. Sci. Technol. B* **3**, 724 (1985).
- [19] R. Venkatasubramanian, E. Siivola, T. Colpitts, and B. O’Quinn, *Nature (London)* **413**, 597 (2001).
- [20] S. Cho, Y. Kim, A. DiVenere, G. K. Wong, J. B. Ketterson, and J. R. Meyer, *Appl. Phys. Lett.* **75**, 1401 (1999).
- [21] L. W. da Silva, M. Kaviani, and C. Uher, *J. Appl. Phys.* **97**, 114903 (2005).
- [22] G. Wang, L. Endicott, and C. Uher, *Sci. Tech. Adv. Mater.* **3**, 539 (2011).
- [23] P. Janicek, C. Drasar, L. Benes, and P. Lošt’ák, *J. Electron. Mater.* **39**, 1814 (2010).
- [24] See Supplemental Material at <http://link.aps.org/supplemental/10.1103/PhysRevLett.111.046803> for calculations of lattice mismatch and phonon mean-free path.
- [25] J. M. Underwood, P. J. Lowell, G. C. O’Neil, and J. N. Ullom, *Phys. Rev. Lett.* **107**, 255504 (2011).